Spectroscopy of non-interfering photons through nonlinear integrated optics Mach-Zehnder interferometer

Chiarini, Marco, Bentini, Gian , Desalvo, Agostino

Marco Chiarini, Gian G. Bentini, Agostino Desalvo, "Spectroscopy of non-interfering photons through nonlinear integrated optics Mach-Zehnder interferometer," Proc. SPIE 10230, Quantum Optics and Quantum Information Transfer and Processing 2017, 1023004 (16 May 2017); doi: 10.1117/12.2265742

SPIE.

Event: SPIE Optics + Optoelectronics, 2017, Prague, Czech Republic

Spectroscopy of non-interfering photons through non-linear integrated optics Mach-Zehnder interferometer

Marco Chiarini*[a], Gian G. Bentini[b], Agostino Desalvo[b]
[a]Prometheus S.r.l., c/o CNR-IMM, Via P. Gobetti 101, 40129 Bologna, Italy;
[b]Consiglio Nazionale delle Ricerche – Istituto per la Microelettronica e i Microsistemi, Via P. Gobetti 101, 40129 Bologna, Italy

ABSTRACT

Quantum optics has become a key field of development for investigations of quantum physics principles, leading to novel quantum technologies. In this view Integrated Optics allows implementing complex quantum circuits that can give rise to significant outcomes, difficult to reach using traditional approaches based on discrete components. In this framework, a non-linear Mach-Zehnder Interferometer (MZI) was implemented by using two commercial 50:50 directional fibre couplers. One of the MZI arms was equipped with a single mode Er:$LiNbO_3$ optical waveguide, acting as non-linear component whereas the other MZI arm was provided with an undoped $LiNbO_3$ single mode optical waveguide, used to obtain a phase shift through the application of a controlled voltage ramp. The injection in the MZI of a 980nm wavelength laser radiation allowed to collect structured interferogrammes, that could be ascribed exclusively to the pump photons, as all frequency conversion events are localized only in one arm of the Interferometer. The Fourier Transform elaboration of such interferogrammes, produces multiple peak spectra that tightly match the typical transition spectrograms of Er:$LiNbO_3$ when excited by a 980nm radiation. Thus it is possible to perform a spectrometry of the non-interfering converted photons only by using the interfering pump photons.

In this work, the experimental apparatus and the most interesting results, obtained in different experimental conditions, are described. Finally, a possible interpretation is outlined.

Keywords: Quantum Technology, Quantum States Characterization, Integrated Optics and Photonics for Quantum Physics, Fourier Transform Spectroscopy, Micro Electro Optical Systems Technology, LiNbO3 Technological Platform, Non-linear Mach-Zehnder Interferometer.

1. INTRODUCTION

Since the last decades, interferometric devices started playing a basic role in the experimental study of several basic phenomena[1,2].

Most of the experimental set-ups are based on the two ways Mach-Zehnder interferometer, and on variations of this geometry[2-4]. Almost all the experimental set-ups are implemented in a "traditional" way, i.e. the photons mainly travel in air, at a speed v independent of λ ($v \sim c$). On the contrary, in the case of photons propagating in a medium the propagation speed depends on λ, i.e. $v=v(\lambda)=c/n(\lambda)$. In particular, this situation can become relevant in case a nonlinear optical element is placed inside the interferometer optical paths, in this case, in fact, a frequency conversion of a fraction of the pump photons can take place, generating new photons. Consequently, phase shifts arising from the different wavelength of the generated photons, are introduced in the photons flux as a function of the optical path length.

In the present work we studied the importance of the above described phase shift in connection with fringe visibility for a monochromatic input, when phase shifters are placed in the arms of a Mach-Zehnder interferometer[4].

Nowadays, an integrated optics approach appears necessary for practical applications and can become useful also for fundamental studies of quantum optics[5,6].

*chiarini@bo.imm.cnr.it; phone +390516399153; fax +390516399216.

Quantum Optics and Quantum Information Transfer and Processing 2017, edited by Konrad Banaszek, Christine Silberhorn
Proc. of SPIE Vol. 10230, 1023004 · © 2017 SPIE · CCC code: 0277-786X/17/$18 · doi: 10.1117/12.2265742

In particular, when propagation takes places in a single mode optical waveguide, all transmitted photons are in a spatial coherent state[7].

Solid state interferometers can be fabricated with integrated optics techniques as well as with a hybrid set-up composed by optical fibres and monolithic optical waveguides. In these devices, photons of different wavelength can be delivered through the interferometer and generate interference patterns containing information on the phase shifts produced in different photon groups, propagating at different speeds.

In the last decade, our research group has reached a remarkable experience in the fabrication of high performance Integrated Mach-Zehnder Interferometers (IMZ) to be used as Fourier Transform Spectrometers[8-13].

In the present work we applied both integrated optics and Fourier Transform Analysis to perform an experiment that can be relevant for fundamental quantum optics studies. This is a rather novel approach that can be used because in quantum mechanics the wave functions of two conjugate variables are Fourier Transform pairs. In fact, operating in the Fourier Transform time-frequency space domain, we are able to recover the spectral composition, in the wavenumber space, of the photons generated by the excitation of an Er^{3+} doped nonlinear crystal placed in one arm of the interferometer.

2. EXPERIMENTAL AND RESULTS

Figures 1 and 4 show the experimental apparatus that was implemented.

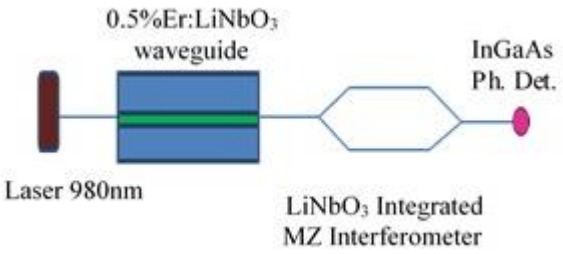

Figure 1. Layout used for the preliminary measurement of the spectral composition generated by the Er^{3+} doped waveguide, excited by a 980nm laser source.

The spectrum excited by the laser pump in the Er^{3+} doped waveguide, was preliminary measured by means of the set-up of Figure 1. In particular, a 0.5% Er:$LiNbO_3$ waveguide was inserted in between the laser source and a monolithic IMZ[10], used as a Fourier Spectrometer, in combination with an InGaAs Photodetector (operative in the 400-1700nm spectral window). The result of the interferometric measurement and of the corresponding spectrum obtained by Fast Fourier Transform, (FFT), joined to successive calibration on the Photodetector spectral response is reported in Figure 2. For comparison, in Figure 3 is reported the absorption spectrum of Er:$LiNbO_3$, showing the major peaks, as reported in the literature[14].

Once the spectral composition generated by the Er^{3+} doped crystal was known, we prepared a Mach-Zehnder interferometric apparatus composed by two 50:50 directional single mode fibre couplers connected with "Pigtail" technique to two monolithic single mode waveguides fabricated by Ion Implantation on a X-cut $LiNbO_3$ substrate.

The fabrication process of the $LiNbO_3$ waveguides is reported in refs. [10] and [15] and the experimental set up is sketched in Figure 3, where the monolithic wave guides are inserted each in one of the two arms of the interferometer, respectively. This way, the Er^{3+} doped arm, (c), acted as a nonlinear optic element suitable to generate photon conversion, whereas the second undoped arm, (d), is used as phase shifter.

This apparatus can be considered as a hybrid solid-state version of the Asymmetric Non Linear Interferometer, (ANLI), described in ref. [3], thus behaving as a source of Maximally Entangled States, (MES), over the two modes of the Mach-Zehnder. In order to generate the controlled optical path variation using the electro-optic properties of the $LiNbO_3$ base material, the undoped arm, (d), was equipped with two driving electrodes, photo-lithographically deposited on the optical chip.

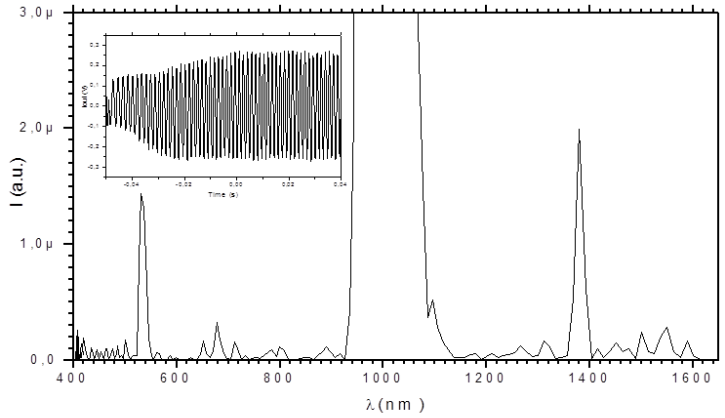

Figure 2. Spectral response obtained with the Fast Fourier Transform, (FFT) analysis showing the laser pump peak (980nm) together with the well-known family lines around 500 nm, 700 nm, 1390 nm and 1550 nm, typical of a Er^{3+} doped waveguide, obtained with an InGaAs photodetector.

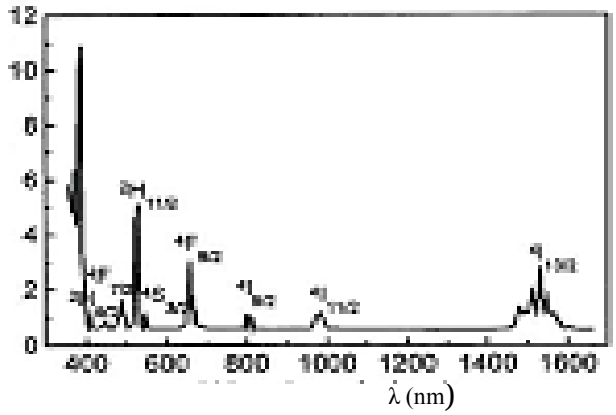

Figure 3. Absorption spectrum of Er^{3+} doped $LiNbO_3$ as reported in ref. [14].

A stabilized digital voltage ramp was supplied to drive the electric field that allowed us to precisely control the phase shift, ($\Delta\varphi$), between the two arms of the interferometer[15].

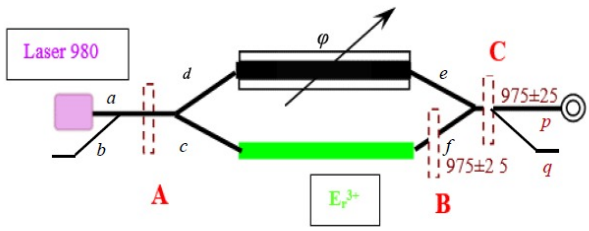

Figure 4. Schematics of the layout used for the present experiment. The dotted areas indicate the different positions where a filter at (975±25) nm was placed in different moments of the experiment, (see text).

This experimental arrangement offers the possibility both to insert, with a plug and play process, wavelength filters in the desired positions along the optical paths, and to balance the signal intensities of the two arms, so optimizing the signal to noise ratio in the interferogramme. Furthermore, dealing with single mode radiation, it was possible to always work with very well spatially confined coherent photons, giving rise, at the exit coupler, both to a high degree of mode matching and to a fast collection of high quality experimental data.

Moreover, unlike continuous variable path-length systems based on piezoelectric stretching of the optical fibres[7], the present experimental set-up allowed a $\Delta\varphi$ variation corresponding to an optical path difference of many hundreds of wavelengths in the in the undoped arm of the interferometer. This figure is fundamental in the development of the present experimental work and is not easily attainable with other methods.

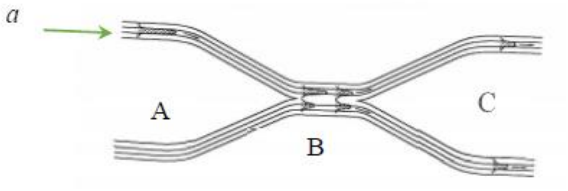

Figure 5. Sketch of the behaviour of the symmetric coupled junction.

The behaviour of the photons propagating in a lossless symmetric coupled Y-junction has been widely treated in the literature[16-18] and consequently will not be discussed here in detail, nevertheless, it is worth making some comments on the use of optical fibre coupled junction playing in this case the role played by the beam splitters in usual Mach-Zehnder interferometers.

Observing the schematic drawing[18] reported in Figure 5, we simply notice that the two single-mode fibres, forming the entrance port, are coupled in close proximity to allow the transfer of a fixed amount of energy between the two fibres. Figure 5 displays a sketch of a single mode laser radiation arriving to the symmetric coupled junction. The fields propagating in the coupling region, (B), develop a relative phase difference, ($\Delta\varphi$), that changes with the distance of propagation. When the propagation distance is $z = \pi/(2H)$, (were H is a constant characteristic of the coupling), the phase shift becomes $\pi/2$, so the photons equally split in the two arms ideally in phase. In this view, we can consider that the introduction of a fibre coupler in the optical circuit has the same effect as the introduction of a beam splitter in the port, (a), used for the entrance of the laser field, E(t).

From the Quantum Electrodynamics viewpoint, it is assumed that the input in the lower port in Figures 4 and 5, is a quantum vacuum state[19,20] ,therefore a noise arises from the vacuum field fluctuations. A quantum noise is then produced in the coupled region B, and transmitted to the two arms in region C, giving rise to the fluctuations of the electric field, $\Delta E(t)$ [20,21] .

At the exit ports of the interferometer, the coupling device has exactly the reverse behaviour. The two modes of the IMZ collapse in the coupling region, (B), giving rise to an interference pattern. In particular, when $\Delta\varphi=\pi/2$, antisymmetric modes that are delivered to the exits cancel each other, whereas symmetric modes sum up.

Therefore, for a sufficiently large time controlled optical path difference, and a correspondent phase shift $\Delta\varphi$, it is possible to obtain an experimental interferogramme as a function of time.

As for the detection system, we used both InGaAs and Si p-i-n photodetectors depending on the experimental requests, (see text in the following).

It must be stressed that with the layout of Figure 3, the photons generated in the doped arm of the interferometer cannot contribute to the interference due to the "which way?" criterion.

Once the 980 nm laser pump was injected the entry port (a) of the ANLI device, a 100 V linear voltage ramp was applied to the undoped arm of the interferometer, with a scan frequency of 30 Hz. By Pockels' effect, the linear voltage variation gave rise to a corresponding variation of the refractive index generating, in turn, a continuously variating phase shift between the photon states entangled over the two arms of the interferometer.

The experimental data were collected at one of the two exit ports, (p or q), of the second coupled junction, (that are equivalent apart from a constant phase shift), in form of interferogramme, generated by the intensity measured at the photodetector as a function of time.

In the case in which a non-monochromatic light is injected in the IMZ the interferogramme shows frequency beatings and the Fourier analysis of the interferogramme gives the whole spectrum of the injected radiation. The raw data were corrected using the well-established algorithms currently used in the Fourier Transform spectroscopy[10,12,13,22].

Figures 6 and 7 display the experimental spectra obtained at the exit of the ANLI device. The raw interferogramme is reported in the inset of the figures.

The spectral lines reported in Figs. 6 and 7 were obtained collecting the experimental data with InGaAs and Si p-i-n photodetectors respectively.

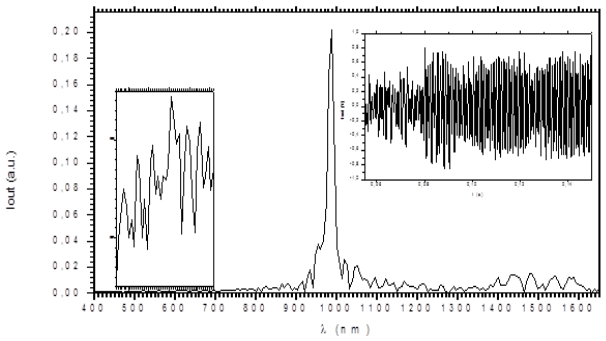

Figure 6. Spectrum obtained by FFT analysis with the experimental set-up of Figure 2, with InGaAs photodetector. The left side inset shows a magnified, (X10), short wavelength part of the spectrum.

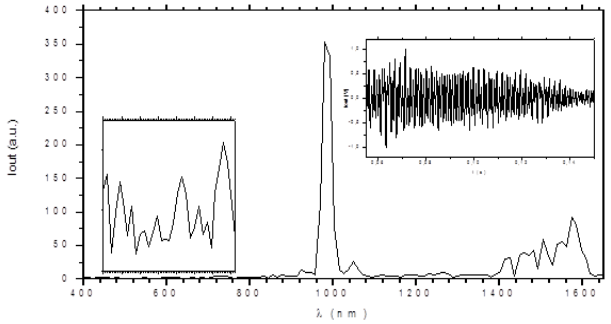

Figure 7. The same conditions of Figure 6 are reported, but with a Si p-i-n detector. The left inset shows the magnified, (X10), short wavelength part of the spectrum. The right side insets show the corresponding interferogrammes. The wavelength filters were inserted in the optical path.

Despite the different spectral responsivity of the applied photodetectors, both detecting systems show the presence of frequency beatings in the corresponding raw output interferogrammes. The consequent FFT analysis gives rise to spectra showing the same most significant peaks for both interferogrammes.

In particular, the FFT analysis of the interferogrammes gives rise to a spectral response having the same spectral lines of the Er: $LiNbO_3$, displayed in Figure 8.

The differences in the intensity of the spectral lines, that are uninfluential for the sake of this work, are originated by the different responsivity of the two detectors.

To eliminate all components different from the laser pump radiation, a dichroic mirror cutting all the short wavelength radiation was inserted before the photodetector. Moreover, with reference to Figure 4, wavelength pass-band filters at (975±25) nm, were placed in the positions A, B and C of the interferometric set up. This wavelength filtering procedure had only the beneficent effect to improve the visibility of the interferogramme beats. In fact, the wavelength filtering

procedure gives rise to noise reduction because it allows only the transmission of the 980 nm pump photons thus cleaning the incoherent background generated in the Er:$LiNbO_3$ doped arm. Furthermore, it must be considered that the Si p-i-n detector is "blind" to I. R. radiation for wavelengths $\lambda \geq 1.1\mu m$, so it could not detect the photons corresponding to the ~1.55μm family peaks present in the spectrum of Figure 6, if any.

In Figures 6 and 7, the short wavelength lines show relatively low intensities because they are generated by a low efficiency multi-photon process. Despite this, the intensity of the family lines grouped around 490-800 nm is still appreciable, whereas the longer wavelength lines, generated by single-photon processes around 1550 nm, are clearly detected.

It can be useful to remember that the fringe visibility, ν, is given by[23]:

$$\nu = \frac{2T}{\left(1+T^2\right)} \text{ where: } T^2 = \frac{\langle c|c\rangle}{\langle d|d\rangle}$$

so, to increase ν, is convenient to work with a balanced value of the intensities of the photons flux in the two arms |c> and |d > of the IMZ.

In Figure 8, the emission lines and the corresponding energy transitions of Er^{3+}, as reported in the literature, are listed.

From the comparison of the experimental data reported in Figures 6 and 7, we can draw a surprising conclusion. Even if in our experimental set-up only the monochromatic, (λ= 980 nm), pump radiation can generate interference and can reach the detector, it is possible to obtain the whole emission spectrum of the Er^{3+} doped component, inserted in the arm c of the interferometer, giving us quantitative information about almost all its energy levels in terms of wavenumber k.

This point will be discussed in detail in the next section. Here we will only stress that, due to the time dependent phase shift induced in the arm d of the ANLI, joined to the Fourier Transform Analysis method, we can obtain the energy level structure of the nonlinear doped crystal, without detecting the photons generated by the interaction with the monochromatic laser pump.

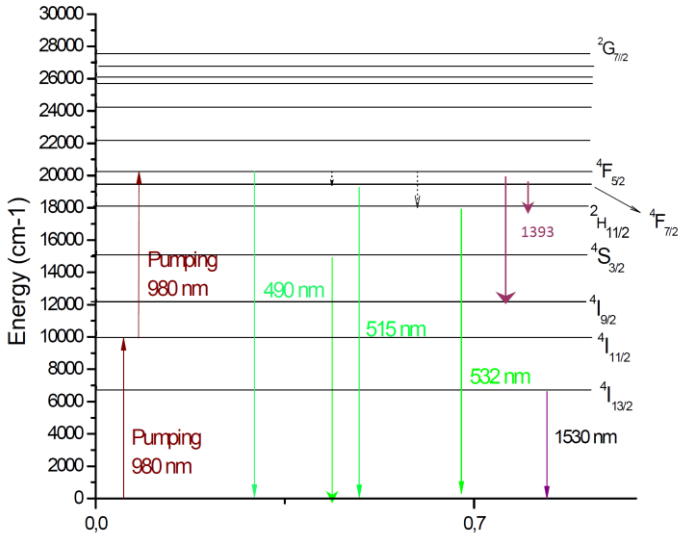

Figure 8. Energy levels of Er^{3+}:$LiNbO_3$.

To further verify the experimental results, we injected in the ANLI a laser diode radiation at λ=1320 nm.

Photons of this wavelength do not produce any excitation of the energy levels of Er^{3+} so, apart the velocity, the propagation behavior inside the material can be considered similar to the propagation in vacuum.

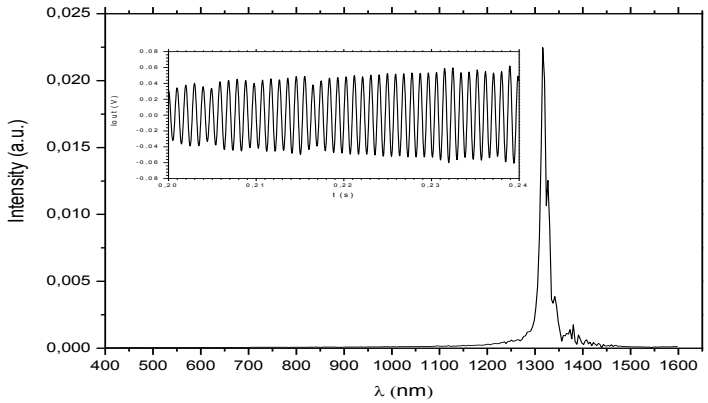

Figure 9 Interferogramme and spectrum obtained injecting the laser beam at 1320 nm

Figure 9 displays the corresponding FFT spectrum only showing the laser diode lines, as we should have observed in vacuum, without any trace of the Er^{3+} spectral lines.

3. DISCUSSION

The experimental results obtained with this measurement, particularly considering that it was performed with the wavelength filters placed in the optical path, demonstrates that the only photons transmitted in the interferometer and reaching the detector are those non interacting with the doped crystal, generated by the 980 nm laser pump. Nevertheless, we observe the spectral lines of the Er^{3+} energy levels.

This result also demonstrates that with an ANLI device, we can perform quantitative physical measurements of undetected photons. In conclusion, all the measurement here described, lead to a positive indication about the possibility to have the experimental spectroscopy of the undetected photons, generated by the nonlinear Optical Element. In fact, in the present experiment, the photons emitted by the dopant cannot contribute to the interferogramme and are removed owing to the use of the (975±25) nm optical filter before the detector. From this point of view, the present result is analogous to the one reported in ref. [2], where undetected photons were used to obtain the shadow image of an object, placed on one arm of the interferometer.

In the present experiment, using annihilation of pump photons, we could obtain quantitative information about the energy states, (spectral lines), of the object. In this case the object is the Er^{3+} dopant of the nonlinear crystal waveguide placed in the arm c of the interferometer.

The present result was made possible because we introduced a controlled time dependent very large phase shift. In fact, the modulation of the interferogramme is originated by the phase shifts of the non-interacting photons entangled with the vacuum states generated by the photon pump annihilation. In this experiment we know "where" the photons annihilate, (the doped arm), but we do not know "when" [26], whereas the photons generated by several processes including up or down conversion in the c arm, are incoherent and only give rise to the experimentally observed background increase.

A further information of the present experimental result, concerns the confirmation that the path entangled states between the two spatially separated modes, are maintained also when the photon propagation takes place in solid dispersive materials without remarkable dissipative de-coherence, as already reported in the literature[5,27,28,29].

In the followings, we will propose a mathematical interpretation showing that the origin of the Er^{3+} spectral lines present in the interferogramme of the pump photons, can be correlated to the annihilation of the pump photons that interact with the Er^{3+} dopant, giving rise to up and/or down conversion processes generating new photons in the visible and near infrared.

In the symmetric configuration of the coupled junction reported in Figure 5, we can write the evolution of the states transmitted through the ANLI.

The balance of the states entering from the ports a, transmitted through the interferometer at the coupler, can be written as:

$$|a\rangle \rightarrow 1/\sqrt{2}\ (i|c\rangle + |d\rangle) \tag{1}$$

where: |a⟩, |c⟩, |d⟩ denote the photons in the different arms of the interferometer and i is the imaginary unit that takes into account the $\pi/2$ phase shift in the coupler.

Taking into account the processes of annihilation and creation of photons, in the arm c we have

$$|c\rangle \rightarrow 1/\sqrt{2}[i\eta(k)|f\rangle_\alpha|f\rangle_\beta + (1-\eta(k))|f\rangle + + \eta(k)|f\rangle_0] \tag{2}$$

where α and β indicate the photons generated as an effect of the pump interaction with the Er^{3+} ions, k is the wavenumber of the generated photons, η(k) is the wavelength dependent probability for any k transition.

The term $\eta(k)|f\rangle_0$ takes into account that for each $|f>_\alpha|f>_\beta$ photonic state, created with η(k) probability by the conversion of a pump photon, there is a corresponding η(k) probability to create a vacuum state |0⟩, originated by the pump photon annihilation [30], [31].

Along the arm d we have

$$|d\rangle \rightarrow 1/\sqrt{2}e^{i\varphi}|e\rangle \tag{3}$$

where φ is the time dependent phase shift introduced by the voltage ramp in the arm d.

One can now write the evolution of the pump states at the exit ports p and q, which can be expressed by the following relationship,

$$|e\rangle \rightarrow 1/\sqrt{2}\ (i|q\rangle + |p\rangle)$$
and
$$|f\rangle \rightarrow 1/\sqrt{2}\ (i|p\rangle + |q\rangle), \tag{4}$$

respectively

Combining eqs. (1)-(4) one obtains

$$|a\rangle \rightarrow \frac{1}{2}[e^{i\varphi}(|p>+i|q>) + i(1-\eta(k))(|q>+i|p>) + \frac{1}{2}i\eta(k)(|q\rangle_\alpha + i|p\rangle_\alpha)(|q\rangle_\beta + i|p\rangle_\beta) + \\ + i\eta(k)(|q\rangle_0 + i|p\rangle_0)] \tag{5}$$

where the symbols have the same meaning as before.

After rather lengthy mathematical manipulations, one obtains for the probability Pp to detect pump photons at the ANLI port p, see Figure 4,

$$P_p \sim \cos^2(\vartheta) + \frac{1}{4}\eta^2(k)\sin^2(\vartheta) \tag{6}$$

where $\vartheta = \varphi/2$.

Owing to the variation of the optical path length originated by Pockels effect applying the electric voltage ramp, the phase $\vartheta=\varphi/2$ varies as a function of the applied electric voltage. Namely,

$$\vartheta = \varphi/2 = \frac{\pi L n}{\lambda} = k\,L\,n/2$$

where, n is the refractive index of the waveguides, L is the length of the electrodes allowing to apply the voltage ramp, and k is the wavenumber.

By integrating over all k, one obtains the following expression:

$$I_{out} \sim \int_0^{\infty} \left(\cos^2(\vartheta) + \frac{1}{4}\eta^2(k) \sin^2(\vartheta) \right) \mathrm{dk} = \text{const.} + \int_0^{\infty} \left(1 - \frac{1}{4}\eta^2(k)\right) \cos(nLk)\ \mathrm{dk} \quad (7)$$

The detailed formal mathematical calculations will be reported in a forthcoming paper. Here we will focus our attention on the physical meaning of terms of Eq. (7).

The first term inside the integral of Eq. (7) is the output interferogramme generated by the pump photons that did not interact with the nonlinear doped element, whereas the last term is the Fourier Transform of the $\eta^2(k)$ term, giving rise to a modulation that sums up to the pump interferogramme, yielding to the frequency beats, evidenced by our experiments.

In particular, the last term is matched to the k vectors and accounts for the annihilation of the pump photons and for the correspondent photons generated through the interaction with the nonlinear medium due to the energy and momentum conservation laws

In fact, due to the presence of the beats, elaborating the interferogramme with the usual Fourier Transform Spectroscopy techniques, we obtain a wavelength spectrum that, contains the laser pump line together with the "ghost" lines generated by the excitation of the Er^{3+} energy levels.

It must be pointed out that, due to the monochromatic nature of the photons transmitted through the ANLI, by elaborating the interferogramme with Fourier spectroscopy techniques, it can be expected that the transition lines characteristic of the energy levels of the doped crystal, can be evidenced as "ghost lines" since they are connected to the annihilation of the pump photons.

In practice due to the continuous phase variation, the process gives rise to the spectral lines produced by the annihilation process, (i.e. $|0\rangle$ states generation), at the same k position corresponding to the Er^{3+} excitation lines. In fact, it must be considered that the pump photons annihilation takes place at well-defined k values fixed by the energy levels of the doped crystal.

It is a matter of fact that the annihilation of the photons that interacted with the nonlinear Er3+ doped crystal gives rise to the E=0 condition of the electric field, ("light switched off"). Furthermore, it is well known[31,32] that, even if $\langle E \rangle = 0$, the electric field intensity, $\langle E^2 \rangle$ and its fluctuation, ΔE, are not zero, (i.e. $\langle E^2 \rangle \neq 0$ and $\Delta E \neq 0$). Therefore, even if the number of photons N becomes equal to 0, the field still have fluctuations, namely the vacuum fluctuations[4,32], (quantic vacuum zero-field fluctuations).

The annihilation of the pump photons that interacted with the nonlinear doped crystal, gives rise to the condition $\langle E \rangle = 0$ of the electric field, consequently, the levels observed in the dimensional space k can be connected to the levels of the quantic vacuum, generated by the zero reset of the electric field by the interaction with the Er^{3+} dopant.

4. CONCLUSIONS

The objective of this work was to present the results of interaction-free measurements allowing to get "ghost" spectroscopic information about an object placed in one arm of an interferometer. The experimental system consists in a hybrid wave-guided solid state device exploiting an integrated quantum photonic circuit that is equivalent to an Asymmetric Nonlinear Mach-Zehnder Interferometer. Here we show that our experimental results could demonstrate, for the first time at our knowledge, the possibility to experimentally extract the structure of the Quantum Vacuum States originated by an Er:$LiNbO_3$ nonlinear optical element, placed in one of the arm of the interferometer and interacting with a 980nm laser pump source. The novelty of this experience resides in the fact that the spectral distribution of the photons converted by Er^{3+} ions, was obtained only by using the pump photons, some of which experience annihilation, without the need to directly detect the photons generated by the conversion processes. This experience opens the way to the development of fast and sensitive interaction-free "Ghost Spectroscopy" techniques.

REFERENCES

[1] Barreto Lemos, G., et al., "Quantum imaging with undetected photons," Nat. Lett. 512(7565), 409-412 (2014).

[2] Du Marchie van Voorthuysen, E. H., "Realization of an interaction-free measurement of the presence of an object in a light beam," Am. J. of Phys. 64(12), 1504-1507 (1996).

[3] Gerry, C. C., Benmoussa, A. and Campos, R. A., "Nonlinear interferometer as a resource for maximally entangled photonic states: Application to interferometry," Phys. Rev. A 66(1), 013804 1-8 (2002).

[4] Demtröder, W., "Amplitude and Phase Fluctuations of a Light Wave," Laser Spectroscopy 2, 577-581, Springer Verlag Berlin, (2015).

[5] Politi, A., Matthews, J. C. F., Thompson M. G., and O'Brien, J. L., "Integrated Quantum Photonics," IEEE J. Sel. Top. Quant. Electron. 15(6), 1673-1684 (2009).

[6] O'Brien, J., Brian, P., Sasaki, M., and Vuckovic, J., "Focus on Integrated Quantum Optics," New J. of Phys. 15, 035016 1-3 (2013).

[7] Kaiser, F., Fedrici, B., Zavatta, A., D'Auria, V., and Tanzilli, S., "A fully guided-wave squeezing experiment for fiber quantum networks", Optica 3(1), 362-365 (2016).

[8] Bentini, G. G., et al., "Effect of low dose high energy O^{3+} implantation on refractive index and linear electro-optic properties in X-cut $LiNbO_3$: Planar optical waveguide formation and characterization," J. of Appl. Phys. 92(11), 6477-6483 (2002).

[9] Bentini G. G., et al., "Damage effects produced in the near-surface region of x-cut $LiNbO_3$ by low dose, high energy implantation of nitrogen, oxygen and fluorine ions," J. of Appl. Phys. 96(1), 242-247 (2004).

[10] Bentini G. G., et al., "Integrated Mach-Zehnder micro-interferometer on $LiNbO_3$," Optics & Laser in Eng. 45(3), 368-372 (2007).

[11] Bentini G. G., et al., "Modification of the etching properties of x-cut Lithium Niobate by Ion Implantation," Nucl. Instr. and Meth. in Phys. Res. B 266(8), 1238–1241 (2008).

[12] Li, J., Lu, D., and Qi, Zh., "Miniature Fourier transform spectrometer based on wavelength dependence of half-wave voltage of a LiNbO3 waveguide interferometer," Opt. Lett., 39(13), 3923-3926 (2014).

[13] Bentini, G. G., and Chiarini, M., "Integrated Optical Microsystems for Interferometric Analytics, Optical Nano-Microsystems for Bioanalytics", 103-153, Fritzsche, W., and Popp J., Ed., Springer Verlag Berlin (2012).

[14] Zheng, J., et al., "Visible dual-wavelength light generation in optical superlattice Er:$LiNbO_3$ through up conversion and quasi-phase-matched frequency doubling," Appl. Phys. Lett. 72(15), 1808-1810 (1998).

[15] Kok, P., Lee, H., and Dowling, J. P., "Creation of large-photon-number path entanglement conditioned on photo-detection," Phys. Rev. A 65(5), 052104 1-5 (2002).

[16] Love, J. D., and Riesen, N., "Single-Few-and Multimode Y-Junctions," J. of Lightw. Tech. 30(3), 304-309 (2012).

[17] Little, B. E., and Huang, W. P., "Coupled-Mode Theory for Optical Waveguides," Progress in Electromagnetics Research 10, 217-270 (1995).

[18] Wilson J., and Hawkes, J., "Optoelectronics: an Introduction," Prentice Hall Europe (1998).

[19] Coles, P. J., Kaniewski, J., and Wehner, S., "Equivalence of wave–particle duality to entropic uncertainty," Nat. Comm. 5(5814), 1-8 (2014).

[20] Weihs, G., and Zeilinger, A., "Photon statistics at beam splitters: an essential tool in quantum information and teleportation, Coherence and Statistics of Photons and Atoms," Perina, J., Ed., Wiley and Wiley (2001).

[21] Zeilinger, A., "General properties of lossless beam splitters in interferometry," Am. J. Phys. 49(9), 882-883 (1981).

[22] Li, J., Lu, D., and Qi, Zh., "A Modified Equation for the Spectral Resolution of Fourier Transform Spectrometers," J. of Lightw. Tech. 33(1), 19-23 (2015).

[23] Englert, B. G., "Fringe Visibility and Which-Way Information: An Inequality," Phys. Rev. Lett. 77(11), 2154-2157 (1996).

[24] Jeng, Ch., Chen, J., and Sheu, W., "Green up conversion emission of an Er-doped fiber pumped with infrared Laser," Proceeding of the "2008 International Conference in Optics and Photonics", vol. 1, Taiwan, 2008.

[25] Ruan, Y., Li, B., Li, W., and Wan, L., "Spectra, energy levels and up-conversion effect of erbium ions in LiNbO3 crystals," Acta Physica Sinica (Overseas edn.) 4(1), 24-32 (1995).

[26] Franson, J. D., "Bell inequality for position and time," Phys. Rev. Lett. 62(19), 2205-2208 (1989).
[27] Rosenberg D., et al., "Long-Distance Decoy-State Quantum Key Distribution in Optical Fiber," Phys. Rev. Lett. 98(1), 010503 1-4 (2007).
[28] Bonneau, D., et al., "Fast Path and Polarization Manipulation of Telecom Wavelength Single Photons in Lithium Niobate Waveguide Devices," Phys. Rev. Lett. 108(5), 053601 1-5 (2012).
[29] Feng, Sh., and Pfister, O., "Quantum Interference of Ultrastable Twin Optical Beams," Phys. Rev. Lett. 92(20), 203601 1-4 (2004).
[30] Brendel, J., Gisin, N., Tittel, W., and Zbinden, H., "Pulsed Energy-Time Entangled Twin-Photon Source for Quantum Communication," Phys. Rev. Lett. 82(1), 2594-2597 (1999).
[31] Greenberger, D. M,. Horne, M. A., and Zeilinger, A., "Multiparticle Interferometry and the Superposition Principle," Physics Today 46(8), 22-29 (1993).
[32] Gerry, C. C., and Knight, P. L., "Quantum fluctuations of a single-mode field, Introductory Quantum Optics," 16, Cambridge University Press (2005).